American Mineralogist, Volume 89, pages 819–831, 2004

Compositional characteristics and paragenetic relations of magnesiohögbomite in aluminous amphibolites from the Belomorian complex, Baltic Shield, Russia

PULAK SENGUPTA,[1] MICHAEL M. RAITH,[2,*] AND VALERI I. LEVITSKY[3]

[1]Department of Geological Sciences, Jadavpur University, Kolkata–700032, India
[2]Mineralogisch-Petrologisches Institut, Universität Bonn, Poppelsdorfer Schloss, 53115 Bonn, Germany
[3]Institute of Geochemistry, Siberian Branch, RAS, Favorski st., 1a, Irkutsk–664033, Russia

ABSTRACT

This study investigates the compositional characteristics, parageneses, and stability relations of some högbomite-bearing assemblages in coarse-grained corundum-garnet amphibolites from a blackwall zone that separates troctolitic metagabbro from kyanite-bearing paragneiss at Diadina Mountain, Belomorian Belt, Russia. The blackwall zone presumably was formed through infiltration driven metasomatism during the Svecofennian metamorphic event at ~1.9 Ga. Euhedral högbomite grains (up to 15 mm in size) occur in domains of coarse tschermakitic amphibole, biotite, and spinel with minor rutile and ilmenite in the two blackwall varieties having contrasting bulk compositions. The other minerals in the two associations include corundum + garnet ± cordierite + chlorite + plagioclase + carbonate and spinel ± gedrite + sapphirine + chlorite + carbonate.

The studied högbomite belongs to the magnesiohögbomite-2*N*3*S* polysome type [$P\bar{3}m1$ with a = 5.721(1) Å, c = 23.045(1) Å] and exhibits compositions that are poor in Zn (0.05–0.42 wt% ZnO) and Ni (0.20–0.50 wt% NiO) [$(Fe^{2+}_{2.7–3.1}Mn_{0.01}Ni_{0.04–0.1}Zn_{0.01–0.1})Mg_{4.8–3.7}(Al_{18.1–18.8}Cr_{0.1–0.2}Fe^{3+}_{0.4–0.9})Ti_{1.6–1.2}O_{38}(OH)_2$]. Compositional variation is controlled by the substitution $Ti^{4+} + R^{2+} \leftrightarrow 2R^{3+}$. Systematic partitioning data for Fe^{2+}, Mg, and Zn indicate attainment of chemical equilibrium between magnesiohögbomite and the associated minerals (Spl, Hbl, Ged, Grt, Spr, Bt) on the thin section scale. Textural relations suggest growth of magnesiohögbomite under amphibolite-facies conditions (6 ± 1 kbar, 600 ± 50 °C) through complex mineral-fluid equilibria involving oxide (Crn, Spl, Rt, Ilm), silicate (Am, Bt, Spr), and carbonate (Cal, Dol, Mgs) phases. A partial $\log f_{O_2}$-$\log f_{S_2}$ diagram for the system FeO-Al_2O_3-TiO_2-O_2-S_2-H_2O shows that growth of magnesiohögbomite from Crn + Ilm and Spl + Rt is restricted to a narrow f_{O_2}-window and low f_{S_2}. The topological constraints, together with petrological data, suggest that magnesiohögbomite is formed in titanian and aluminous protoliths under greenschist-to amphibolite-facies conditions if f_{H_2O} is high, f_{S_2} low, and f_{O_2} is defined by the paragenesis ilmenite + rutile + magnetite.

INTRODUCTION

Högbomite-group minerals are complex Fe-Mg-Al-Ti oxides related to the spinel group but differing from it by having significant TiO_2 and structural water (reviewed in Grew et al. 1987, 1990; Petersen et al. 1989; Hejny and Armbruster 2002). They are characterized by a modular structure composed of spinel ($T_2M_4O_8$) and nolanite [$TM_4O_7(OH)$] units and, depending on the stacking periodicity of the modules, form various polysomes (Hejny and Armbruster 2002; Armbruster 2002). Once thought to be rare, högbomite has been reported from Fe-Ti ores and aluminous amphibolites of over 57 localities (reviewed in Petersen et al. 1989 and Razakamanana et al. 2000), where it dominantly occurs as a fine-grained mineral intimately related to spinel and magnetite. To our knowledge, the association högbomite–sapphirine has been unequivocally reported from only three areas (i.e., Greenland: Ackermand et al. 1983; Norway: Visser et al. 1992; Greece: Liati and Seidel 1994). Owing to its small grain size, the commonly observed disequilibrium relations with the associated phases, the complex stacking sequence of the structure, and the site occupancy and intercrystalline cation distribution with the associated silicates and oxide phases are poorly understood. Because of these shortcomings, the controls of pressure, temperature, fluid and bulk compositions on the stability of högbomite-bearing assemblages are elusive (cf., Grew et al. 1987; Petersen et al. 1989). Existing information, mostly retrieved from the stability relations of the associated minerals, suggests the formation of högbomite within a restricted temperature range (600 ± 100 °C) but over a wide range of pressures (4–10 kbar) (cf., Ackermand et al. 1983; Coolen 1981; Grew et al. 1987, 1989, 1990; Petersen et al. 1989; Visser et al. 1992; Liati and Seidel 1994; Razakamanana et al. 2000). Grew et al. (1990) have pointed out that the textural relations described for many areas suggest that högbomite formed at lower *P-T* conditions than indicated by the associated silicate and oxide assemblages. This observation stresses the need to study the mutual relations of högbomite with the associated phases before correlating the physical conditions construed from the latter with the genesis of högbomite.

In this paper, we present the textural relations and compositional data of högbomite from a suite of sapphirine- and garnet-bearing aluminous and titaniferous amphibolites of the

* E-mail: m.raith@uni-bonn.de

Belomorian complex, Baltic shield, Russia. Integrating the petrological data, an attempt has been made to elucidate: (1) the compositional variations and the nature of substitutions in högbomite as a function of the associated phases; (2) the mineral reactions leading to the formation of högbomite in different compositional domains; and (3) the stability relations of the högbomite-bearing assemblages in terms of *P-T*-fluid conditions.

Geological background

Corundum-bearing rocks of metasomatic origin, including the högbomite-bearing varieties, are known from several occurrences within the Belomorian Belt (Terehov and Levitsky 1991), a high-grade terrane that was accreted to the northeastern margin of the Karelian Province during the late Archaean (Gaál and Gorbatschev 1987; Gorbatschev and Bogdanova 1993; Bogdanova and Bibikova 1993). The internal architecture of the belt is characterized by NW-trending linear units of psammitic to pelitic gneisses, a high proportion of mafic metavolcanics, and abundant tonalitic to granodioritic orthogneisses (2.8–2.7 Ga), which are interpreted to have resulted from recumbent folding and thrusting of unrelated supracrustal and plutonic lithologies

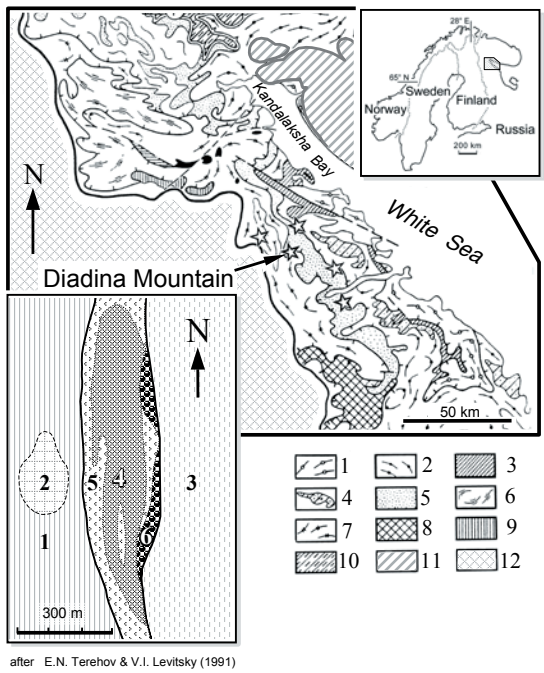

Figure 1. Geological map of the Belomorian Belt in the White Sea area (after Glebovitsky et al. 1996). 1 = Keretz nappe, 2 = Chetolambin nappe, 3 = mafic rocks of the Chetolambin nappe, 4 = Archaean supracrustal rocks of the Pongoma and Gridino area, 5 = Chupa nappe, 6 = Orijärvi nappe, 7 = Kovdozero nappe, 8 = Masdozero nappe, 9 = Archaean greenstone association of the Kovdozero nappe, 10 = Rikolabvino nappe, 11 = Proterozoic nappe units of the Lapland-Kola Orogen; 12 = Karelian Province. Occurrences of corundum-bearing blackwall rocks are shown by stars. The inset shows a simplified geological map of the Diadina locality (after Terehov and Levitsky 1991). 1 = banded migmatite, 2 = two pyroxene-plagioclase gneiss, 3 = aluminous gneiss, 4 = metagabbro (Drusite), 5 = medium to coarse-grained metasomatic garnet amphibolite with högbomite-bearing variants, 6 = metasomatic corundum-garnet rocks.

onto the Karelian cratonic foreland at ca. 2.65–2.6 Ga (Bogdanova and Bibikova 1993) (Fig. 1). The Belomorian terrain was intruded by numerous mafic-ultramafic and charnockitic-syenitic complexes at ca. 2.43–2.4 Ga, when a major phase of crustal extension and rift-related magmatism affected the Karelian and Lapland-Kola cratonic domains. Major parts of the Belomorian Belt were again intensely deformed and overthrust in the northeast by the Kolvitsa-Lapland nappe units during the SW-directed Svecofennian collisional orogeny at ca. 1.9–1.8 Ga. This event caused a regional-scale, amphibolite-facies overprint with formation of abundant muscovite pegmatites (Bibikova et al. 2001).

The corundum-bearing rocks occur exclusively in the contact zones of mafic rocks with their felsic to psammo-pelitic country gneisses and migmatites and, as indicated by their peculiar chemical and mineralogical features, were formed as a result of infiltration-driven metasomatic interaction between the contrasting lithologies. A brief account on the geological setting and petrography of six occurrences was given by Terehov and Levitsky (1991). The högbomite-bearing samples studied in the present contribution come from the Diadina Mountain locality. Here an elongate, ca. 1.2 km long and 200 m wide drusite body (= troctolitic metagabbro with spectacular coronitic reaction rims replacing olivine where in contact with calcic plagioclase) occurs within the high-strain zone between kyanite-bearing paragneisses of the Chupa nappe (to the east) and migmatitic granitoid gneisses of the Kotozero nappe (to the west) (Fig. 1). The metagabbroic body is separated from the country rock gneisses by an up to 100 meters wide zone of garnet amphibolites that, according to Terehov and Levitsky (1991), were formed through amphibolite-facies hydration of the gabbroic body during the late Archaean tectono-thermal event at ca. 2.65 Ga. At the contact with the aluminous gneisses, the garnetiferous amphibolites give way to a blackwall zone of dominantly coarse-grained, corundum-garnet-amphibole rocks and a variety of metasomatic rocks with high-variance mineral assemblages (gedrite, kyanite-gedrite, sapphirine-garnet, garnet, corundum-amphibole, biotite-staurolite-corundum). In the coarse-grained metasomatic domains, högbomite (locally up to 10–15 vol%) was found with two or more of the phases spinel, sapphirine, garnet, cordierite, gedrite, chlorite, and carbonates. Kornerupine and tourmaline have been reported from some places of this zone (Terehov and Levitsky 1991). However, the latter phases were not observed in the studied specimens and their relationship with högbomite is not known. The formation of the blackwall rocks and their textural and paragenetic modifications through recrystallization and retrogression at Diadina Mt. and the other Belomorian occurrences are related to the Svecofennian metamorphic event at c. 1.9 Ga (Terehov and Levitsky 1991; Serebriakov and Aristov 1999; Serebriakov et al. 2001).

Mutual relations among the minerals

In the following sections, textural relations involving högbomite will be elaborated and interpreted to put constraints on the physico-chemical environment upon the growth of this interesting Fe-Mg-Al-Ti oxide. On the basis of the nature and abundance of the coexisting minerals, two högbomite-bearing associations have been recognized:

A (garnet-bearing) – Högbomite + calcic-amphibole + co-

rundum + cordierite + garnet + chlorite + biotite + dolomite + calcite + ilmenite + rutile ± plagioclase ± spinel

B (sapphirine and gedrite-bearing) – Högbomite + calcic-amphibole + gedrite + spinel + sapphirine + magnesite + calcite + ilmenite + rutile + chlorite + biotite

Minerals in both associations are coarse-grained and, with the exception of coronitic garnet in association A, form a granoblastic fabric. The coarse grain size and changes in the modal abundance of the phases on the hand-specimen scale make the estimation of the bulk compositions difficult. However, the distribution of the minerals and their compositions suggest that garnet-bearing association A is Fe rich compared to the sapphirine + gedrite-bearing association B. Unlike most of the known occurrences (reviewed in Grew et al. 1987, 1989, 1990; Petersen et al. 1989; Razakamanana et al. 2000), the studied högbomite assemblages are devoid of magnetite, commonly exclude spinel but coexist with garnet in many cases (in association A).

In association A, högbomite occurs as large platy grains of honeycomb color within a matrix of coarse calcic-amphibole and biotite (Fig. 2A). The euhedral shape of the grains, together with their random orientation, indicates growth and textural equilibration of these three minerals under broadly static conditions. The högbomite grains commonly contain inclusions of rutile and less commonly ilmenite (Fig. 2A). Inclusions of these minerals are also noted in the associated calcic-amphibole and biotite. Corundum porphyroblasts presumably belonged to the matrix assemblage but now occur as relics within complex reaction domains that are made up predominantly of coronal garnet rimming corundum, calcic-amphibole and biotite (Fig. 2B). Cordierite, chlorite, and carbonate (both calcite and dolomite)—with or without plagioclase—also developed in these domains and replace the coarse calcic-amphibole (Fig. 2B and 2C). With the exception of rare inclusions in coronal garnet, högbomite is absent and rutile and ilmenite occur instead. Reaction textures in the narrow transitional zone that separates the corundum-bearing domains from the calcic-amphibole + biotite + högbomite matrix document replacement of högbomite by ilmenite and corundum (Fig. 2D).

The earliest recognizable minerals in association B include calcic-amphibole, spinel, rutile, and locally ilmenite. The last three phases occur as inclusions in the calcic-amphibole, suggesting that they are paragenetically older than the latter mineral. The textural relations, however, do not rule out the possibility that this association was also derived from a corundum-bearing assemblage like that characteristic of association A. The coarse grains of calcic-amphibole are commonly replaced (together with spinel) by an intergrowth consisting of two or more of the phases gedrite, sapphirine, högbomite, calcite, magnesite (Figs. 3A to 3D). Locally, chlorite is also noted in the intergrowths. Inclusions of rutile and ilmenite are common in the högbomite grains. The sapphirine + högbomite intergrowths (plus chlorite) appear to replace spinel near coarse gedrite in some calcic-amphibole-free domains (Fig. 3D). Magnesite is a common carbonate in these domains. However, in many places, chlorite and magnesite also replace sapphirine and gedrite in the absence of högbomite.

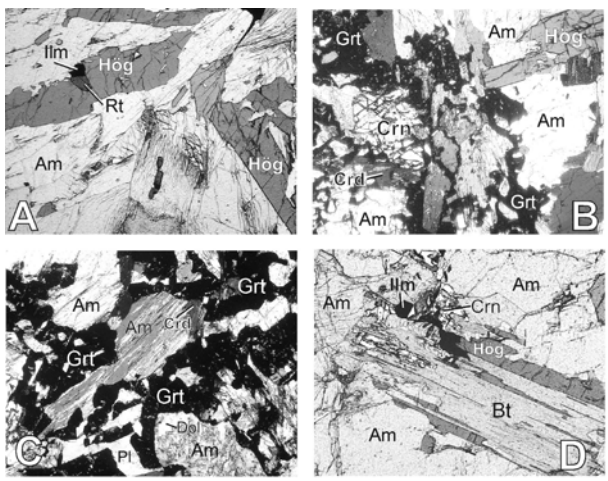

FIGURE 2. Photomicrographs illustrating textural relations in association A rocks from the Diadina occurrence. A = Large högbomite crystals (Hög) randomly intergrown with calcic-amphibole (Am). Note the inclusions of rutile (Rt) and ilmenite (Ilm) in högbomite; B = Isolated corundum grain (Crn) (partly scooped out) in a matrix of coarse calcic-amphibole and högbomite. Coronal garnet (Grt) rims most of the phases. Associated cordierite (Crd) replaces calcic-amphibole; C = Coronal garnet developed around calcic-amphibole and is intergrown with cordierite and plagioclase (Pl). Cordierite and dolomite (Dol) are replacing the amphibole grains at the contact of coronal garnet; D = Intergrowth of högbomite, biotite (Bt) and calcic-amphibole showing replacement by corundum and ilmenite (Ilm); Widths of photomicrographs = 3.4 mm (A) and 1.72 mm (B–D).

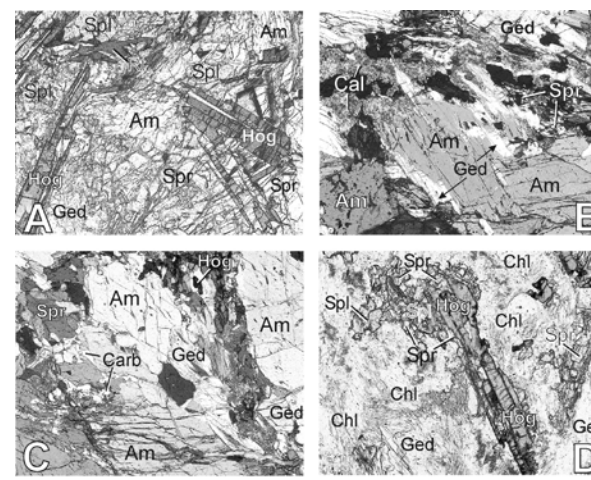

FIGURE 3. Photomicrographs illustrating textural relations in association B rocks from the Diadina occurrence. A = Random högbomite crystals (Hög) intergrown with sapphirine (Spr), biotite (Bt) and gedrite (Ged) replacing calcic-amphibole (Am) and Spinel (Spl). Note the presence of rutile (Rt) in spinel and sapphirine; B = Coarse calcic-amphibole grains are separated from spinel by an intergrowth of sapphirine (Spr), gedrite (Ged) and calcite (Cal); C = Coarse calcic-amphibole grains are replaced marginally by högbomite, sapphirine, gedrite, calcite and magnesite (Carb). D = Spinel is replaced by an aggregate of högbomite, sapphirine, chlorite(Chl) and magnesite (Mag) near gedrite (Ged). Widths of photomicrographs = 3.4 mm (A) and 1.72 mm (B–D).

Mineral chemistry

The compositions of the mineral phases have been analyzed at the Mineralogisch-Petrologisches Institut, University of Bonn, with a CAMECA Microbeam electron microprobe using synthetic and natural standards. Details of the operating conditions are described in Sengupta et al. (1999). Some högbomite grains were analyzed for Sn and Ni with a JEOL SX8900 Superprobe at the Institute for Mineralogy and Geochemistry, University of Cologne, using cassiterite and synthetic NiO as standards. Representative analyses of the different mineral phases are given in Tables 1–4.

Compositional characteristics of phases accompanying högbomite

Garnet in most domains is essentially a solid solution of pyrope and almandine [$Mg/(Mg + Fe^{+2}) = 0.26–0.52$] with low contents of spessartine (≤3 mol%) and grossular (<11 mol%). In some plagioclase-rich domains, the amount of grossular increases to 23 mol% (Table 1). In many domains, garnet shows a strong rimward decrease in pyrope component (commonly more than 10 mol%) at the contacts with ferromagnesian phases like amphibole, biotite, chlorite, spinel, and högbomite (Table 1). However, only a minor rimward decrease in Mg (2 mol%) is present when the mineral surrounds the non-ferromagnesian phases corundum and rutile.

Sapphirine exhibits very magnesian compositions [$Mg/(Mg + Fe^{+2}) > 0.90$] close to the 7:9:3 end-member in terms of $(Fe^{+2},Mg)O:(Al,Cr)_2O_3:SiO_2$ (Table 1). The recalculated Fe^{+3} contents (using charge-balance constraints) give Fe^{+3}/Fe^{+2} ratios > 0.35. Individual grains are compositionally homogenous. Compositions similar to those of the sapphirine studied here were reported from two sapphirine-högbomite occurrences in Norway (Visser et al. 1992) and West Greenland (Ackermand et al. 1983).

Spinel is dominantly a solid solution of hercynite and pleonaste with insignificant contents of Mn, Ti, and Zn components (Table 1). The recalculated Fe^{+3} contents are low (≤0.3 per 3 cations). Spinel grains in association B contain significant Cr_2O_3 (3.61–5.63 wt%) and are more magnesian ($X_{Mg} > 0.59$) than those in the garnet-bearing association A (<0.6 wt% and $X_{Mg} \sim 0.42$ respectively, Table 3). Spinel grains are more magnesian at the contacts with garnet and högbomite than those associated with sapphirine and gedrite (in association B). The calculated Fe^{+3}/Fe^{+2} ratio in spinel is lower than that of the coexisting sapphirine (Table 3).

Cordierite shows a uniform magnesian composition in all the associations ($X_{Mg} = 0.83–0.84$) (Table 2). The alkali contents are low ($Na_2O < 0.05$ wt%). Analytical totals between 98–99 wt% suggest low contents of fluid species in the channels of the structure.

Biotite in both associations is also magnesian ($X_{Mg} \sim 0.88$) with low TiO_2 (< 1.5 wt%) and insignificant Zn and F contents (Table 2).

Chlorite is clinochlore with X_{Mg} and ^{IV}Al varying in the range of 0.69–0.80 and 1.73–2.99, respectively. The mineral is more magnesian and distinctly less aluminous in association B than in association A (Table 2).

Gedrite is magnesian ($X_{Mg} \sim 0.80$) and has ^{A}Na and ^{IV}Al in the range of 0.4–0.5 and 1.8–2.1, respectively (Table 3). The TiO_2 and Cr_2O_3 contents are distinctly lower than in the coexisting calcic-amphibole.

Calcic-amphibole compositions have been recalculated on the basis of 23 O atoms (Table 3), and fall into the field of tschermakite according to the classification of Leake et al. (1997). The mineral shows $X_{Mg} = 0.75–0.86$ with low TiO_2 (<0.9 wt%). The compositions are more magnesian in association B than in the garnet-bearing association A.

Dolomite and magnesite are magnesian carbonates with $X_{Mg} > 0.8$. Corundum and rutile are nearly pure phases. Cr_2O_3 and Fe_2O_3 contents of corundum range up to 0.31 and 0.7 wt%, respectively. Like many low-f_{O_2} rutile+ilmenite-bearing rocks, the compositions of ilmenite are close to the end-member $FeTiO_3$ with insignificant Fe_2O_3 component (<0.5 mol%).

TABLE 1. Electron-microprobe analyses of garnet, sapphirine and spinel

Sample	K136-5	K136-5	K237-10	K237-10		K237-37	K237-37		K237-10	K237-10	K237-37	K237-37
Association	A	A	A	A		B	B		A	A	B	B
Mineral	grt	grt	grt	grt		spr	spr		spl	spl	spl	spl
SiO_2 (wt%)	39.87	39.51	39.14	39.06	SiO_2 (wt%)	13.75	12.97					
TiO_2	0.01	0.02	0.01	0.01	TiO_2	0.04	0.06	TiO_2 (wt%)	0.00	0.00	0.00	0.09
Al_2O_3	22.55	22.52	22.83	21.82	Al_2O_3	62.85	63.16	Al_2O_3	61.92	61.80	59.38	60.48
Cr_2O_3	0.04	0.04	0.04	0.00	Cr_2O_3	0.57	1.38	Cr_2O_3	0.43	0.52	5.63	4.13
FeO	21.56	22.93	19.26	23.43	FeO	4.71	4.56	FeO	26.56	26.40	19.54	19.39
MnO	0.65	0.71	0.46	0.86	MnO	0.01	0.00	MnO	0.05	0.06	0.06	0.11
MgO	10.50	10.36	12.59	11.06	MgO	18.73	18.70	MgO	9.90	10.15	14.71	14.37
CaO	4.87	3.44	5.66	3.42	ZnO	0.00	0.00	ZnO	0.69	0.77	0.44	0.37
Total	100.08	99.55	99.99	99.71	Total	100.10	99.45	Total	99.55	99.70	99.76	98.95
	Formulae normalized to 8 cations				Formulae normalized to 14 cations			Formulae normalized to 3 cations and 4 O atoms				
Si (apfu)	3.01	3.00	2.94	2.98	Si (apfu)	1.61	1.52	Ti (apfu)	0.00	0.00	0.00	0.00
Ti	0.00	0.00	0.00	0.00	Ti	0.00	0.00	Al	1.98	1.97	1.86	1.90
Al	2.00	2.02	2.02	1.96	Al^{IV}	4.39	4.48	Fe^{3+}	0.02	0.02	0.03	0.01
Fe^{3+}	0.00	0.00	0.00	0.00	Al^{VI}	4.26	4.22	Cr	0.01	0.01	0.12	0.09
Cr	0.00	0.00	0.00	0.00	Cr	0.05	0.13	Fe^{2+}	0.59	0.58	0.41	0.42
Fe^{2+}	1.36	1.46	1.21	1.50	Fe^{3+}	0.08	0.13	Mn	0.00	0.00	0.00	0.00
Mn	0.04	0.05	0.03	0.06	Mn	0.00	0.00	Mg	0.40	0.41	0.58	0.57
Mg	1.18	1.17	1.41	1.26	Fe^{2+}	0.38	0.31	Zn	0.01	0.02	0.01	0.01
Ca	0.39	0.28	0.45	0.28	Mg	3.26	3.26					
					Zn	0.00	0.00	X_{Mg}	0.40	0.41	0.59	0.57
X_{Mg}	0.46	0.45	0.54	0.46				Fe^{+2}/Mg	1.47	1.41	0.70	0.74
X_{Mg} Σcat	0.40	0.40	0.45	0.41	X_{Mg}	0.90	0.91	X_{Fe+3}	0.03	0.03	0.06	0.02
X_{Fe+2} Σcat	0.46	0.49	0.39	0.48	Fe^{3+}/Fe^{2+}	0.21	0.43					
X_{Ca}	0.13	0.09	0.15	0.09								
X_{Mn}	0.01	0.02	0.01	0.02								
$X_{Ca}+X_{Mn}$	0.15	0.11	0.16	0.11								

TABLE 2. Electron-microprobe analyses of cordierite, chlorite, biotite, plagioclase and ilmenite

Sample	K237-10	K237-10		K237-10	K237-10	K237-37		K136-5	K237-10		K136-5-18	K237-10-26		K136-5-4	K237-10-4
Association	A	A		A	A	B		A	A		A	A		A	A
Mineral	crd	crd		chl	chl	chl		bt	bt		pl	pl		ilm	ilm
SiO_2 (wt%)	49.31	48.13		26.65	26.47	33.12	SiO_2	38.46	39.17		59.45	57.48	SiO_2	0.02	0.01
TiO_2	0.00	0.01		0.07	0.07	0.18	TiO_2	1.07	0.91		0.00	0.00	TiO_2	52.36	53.48
Al_2O_3	33.88	33.95		23.23	23.10	16.45	Al_2O_3	18.49	19.28		25.80	26.46	Al_2O_3	0.02	0.00
Cr_2O_3	0.00	0.00		0.38	0.24	0.05	Cr_2O_3	0.02	0.08		0.00	0.00	Cr_2O_3	0.09	0.03
FeO	4.13	4.26		14.60	14.02	11.62	FeO	6.09	5.80		0.24	0.19	FeO	46.95	46.44
MnO	0.08	0.05		0.00	0.00	0.05	MnO	0.01	0.02		0.00	0.00	MnO	0.83	0.71
MgO	11.32	11.61		23.28	23.83	25.42	MgO	21.45	22.34		0.00	0.00	MgO	0.07	0.02
CaO	0.03	0.02		0.00	0.00	0.00	Na_2O	0.75	0.64		7.86	8.45	CaO	0.16	0.04
Na_2O	0.04	0.02		0.00	0.00	0.00	K_2O	8.57	8.41		6.84	6.79			
K_2O	0.00	0.00		0.00	0.00	0.00	F	0.16	0.18		0.03	0.03			
Total	98.79	98.04		88.21	87.73	86.88	Total	94.90	96.66		100.21	99.39	Total	100.50	100.73
O atoms	18	18		23	23	23		22	22		8	8		4	4
Si	4.96	4.89	Si	5.26	5.24	6.47	Si	5.46	5.43	Si	2.64	2.59	Ti	1.00	1.01
Al	4.02	4.06	Ti	0.01	0.01	0.03	Ti	0.11	0.10	Al	1.35	1.40	Al	0.00	0.00
Fe^{2+}	0.35	0.36	Al	5.40	5.39	3.78	Al	3.09	3.15	Fe^{3+}	0.01	0.01	Fe^{3+}	0.00	0.00
Mn	0.01	0.00	Cr	0.06	0.04	0.01	Cr	0.00	0.01	Ca	0.37	0.41	Cr	0.00	0.00
Mg	1.70	1.76	Fe^{2+}	2.41	2.32	1.90	Fe^{2+}	0.72	0.67	Na	0.59	0.59	Fe^{2+}	0.98	0.99
Ca	0.00	0.00	Mn	0.00	0.00	0.01	Mn	0.00	0.00	K	0.00	0.00	Mn	0.02	0.01
Na	0.01	0.00	Mg	6.84	7.03	7.39	Mg	4.54	4.62				Mg	0.00	0.00
							Na	0.21	0.17	X_{An}	0.39	0.41			
X_{Mg}	0.83	0.83	X_{Mg}	0.74	0.75	0.80	K	1.55	1.49						
Fe/Mg	0.20	0.21	Fe/Mg	0.35	0.33	0.26	F	0.07	0.08						
							OH	3.93	3.92						
							X_{Mg}	0.86	0.87						
							Fe/Mg	0.16	0.15						

TABLE 3. Electron-microprobe analyses of amphiboles

Sample	K136-5	K136-5	K237-10	K237-10	K237-37	K237-37	K237-37	K237-37
Association	A	A	A	A	B	B	B	B
Mineral	am	am	am	am	am	am	ged	ged
Paragenesis	hög	grt	hög	grt	r-hög,spl	r-ged,spr	hög,spr	hög,spr
SiO_2 (wt%)	43.40	42.69	43.15	42.26	43.99	44.39	45.59	43.84
TiO_2	0.69	0.73	0.75	0.81	0.71	0.71	0.18	0.15
Al_2O_3	17.22	17.34	16.84	17.76	16.45	16.01	16.91	18.76
Fe_2O_3	0.00	0.00	0.00	0.00	0.00	0.00	0.00	0.00
Cr_2O_3	0.06	0.09	0.13	0.13	0.26	0.24	0.17	0.22
FeO	7.21	8.19	6.69	7.68	6.14	6.85	9.26	10.86
MnO	0.02	0.06	0.09	0.05	0.03	0.02	0.09	0.11
MgO	14.82	14.28	15.58	14.70	15.73	15.88	23.23	21.24
CaO	11.62	11.24	11.71	11.74	11.88	11.79	0.57	0.50
Na_2O	1.83	1.54	1.79	1.85	1.52	1.48	1.69	1.98
K_2O	0.25	0.36	0.42	0.45	0.47	0.31	0.00	0.00
Total	97.12	96.52	97.17	97.40	97.19	97.68	97.68	97.66
Formulae normalized to 23 oxygen equivalents								
Si (apfu)	6.107	3.219	6.061	5.956	6.167	6.180	6.309	6.126
Ti	0.073	0.041	0.080	0.085	0.075	0.074	0.018	0.015
Al	2.855	1.541	2.788	2.949	2.718	2.626	2.757	3.090
Fe^{3+}	0.000	0.000	0.000	0.000	0.000	0.000	0.000	0.000
Cr	0.006	0.005	0.015	0.015	0.029	0.027	0.019	0.024
Fe^{2+}	0.849	0.516	0.786	0.904	0.719	0.797	1.072	1.269
Mn	0.003	0.004	0.011	0.005	0.004	0.002	0.010	0.013
Mg	3.107	1.604	3.260	3.085	3.285	3.294	4.789	4.421
Ca	1.751	0.907	1.762	1.772	1.785	1.757	0.084	0.074
Na	0.499	0.225	0.487	0.504	0.413	0.400	0.453	0.537
K	0.044	0.035	0.076	0.080	0.084	0.056	0.000	0.000
X_{Mg}	0.79	0.76	0.81	0.77	0.82	0.81	0.82	0.78
Fe/Mg	0.273	0.322	0.241	0.293	0.219	0.242	0.224	0.287

Compositional characteristics of högbomite

Representative compositions of högbomite in the two associations are presented in Table 4 and their characteristic features are shown in Figure 4. Most of the analyses show totals that are lower than 100%, even when the concentrations of Ni are considered. This is related to the presence of (OH), Fe^{3+}, and other unanalyzed elements like Be.

Recalculation of Fe^{3+} from electron microprobe data requires the knowledge of the polysome type (Armbruster 2002). Each polysome has a characteristic cation sum and element distribution pattern that determines the speciation of Fe from the microprobe data (Grew et al. 1987, 1990; Petersen et al. 1989; Visser et al. 1992; Hejny and Armbruster 2002). Single-crystal data obtained for högbomite of association A sample K237-10 [$P\bar{3}m1$ with a = 5.721(1) Å and c = 23.045(1) Å] indicate a 2*N*3*S*-polysome stacking of spinel and nolanite units (A. Kirfel, personal communication), with close correspondence to the magnesiohögbomite sample from Corundum Creek studied by Hejny and Armbruster

TABLE 4. Electron-microprobe analyses of högbomite

Sample	K136-5	K136-5	K136-5	K136-5	K136-5	K136-5	K136-5	K237-10	K237-10	K237-10	K237-10	K237-10
Association	A	A	A	A	A	A	A	A	A	A	A	A
Paragenesis	crn	crn	rt,ilm	grt	grt	amph	amph	ilm,rt	grt	grt	spl	spl
SiO_2 (wt%)	0.05	0.05	0.01	0.10	0.35	0.03	0.03	0.01	0.03	0.02	0.01	0.02
TiO_2	8.14	8.08	8.08	8.24	8.07	7.79	8.41	8.10	8.20	8.34	6.45	6.34
Al_2O_3	60.39	61.02	61.21	61.88	62.00	62.25	61.80	63.43	62.14	61.88	60.06	61.19
Cr_2O_3	0.42	0.96	1.20	0.96	1.02	0.33	0.49	0.56	0.51	0.47	0.77	0.58
FeO	16.38	16.04	15.92	14.26	14.38	15.52	14.76	14.40	14.58	14.79	20.41	20.33
MnO	0.06	0.00	0.06	0.05	0.02	0.08	0.07	0.09	0.00	0.06	0.01	0.07
MgO	12.36	11.70	12.25	12.70	12.39	12.14	11.57	12.01	12.70	12.81	9.66	9.32
NiO	0.18	0.27	0.32	0.26	0.30	0.16	0.18	0.26	0.20	0.19	0.22	0.27
ZnO	0.05	0.16	0.18	0.16	0.16	0.05	0.05	0.04	0.00	0.00	0.42	0.33
Total	98.04	98.28	99.23	98.61	98.69	98.36	97.36	98.90	98.36	98.56	98.02	98.45
Structural formulae normalized to 28 cations and 78 negative charges												
Si (apfu)	0.012	0.012	0.002	0.026	0.088	0.007	0.007	0.003	0.008	0.006	0.004	0.005
Ti	1.557	1.546	1.530	1.561	1.530	1.481	1.619	1.529	1.554	1.580	1.255	1.227
Al	18.109	18.307	18.165	18.362	18.404	18.536	18.640	18.761	18.454	18.352	18.312	18.563
Cr	0.085	0.193	0.239	0.190	0.203	0.066	0.100	0.111	0.101	0.093	0.157	0.119
Fe^{3+}	0.667	0.382	0.532	0.274	0.157	0.422	0.008	0.064	0.321	0.384	1.014	0.854
Fe^{2+}	2.820	3.033	2.821	2.729	2.872	2.857	3.151	2.959	2.751	2.728	3.403	3.521
Mn	0.013	0.000	0.014	0.010	0.004	0.018	0.015	0.020	0.000	0.012	0.002	0.016
Mg	4.690	4.441	4.599	4.767	4.651	4.571	4.413	4.493	4.770	4.807	3.727	3.576
Ni	0.037	0.055	0.065	0.053	0.061	0.033	0.037	0.052	0.041	0.038	0.046	0.056
Zn	0.010	0.029	0.033	0.029	0.030	0.010	0.009	0.008	0.000	0.000	0.081	0.063
X_{Mg}	0.62	0.59	0.61	0.63	0.61	0.61	0.58	0.60	0.65	0.64	0.51	0.50
X_{Mg} Fe_{tot}	0.57	0.56	0.57	0.61	0.60	0.58	0.58	0.60	0.61	0.61	0.45	0.45
X_{Fe}^{3+}	0.18	0.10	0.15	0.08	0.04	0.12	0.00	0.01	0.16	0.12	0.22	0.19

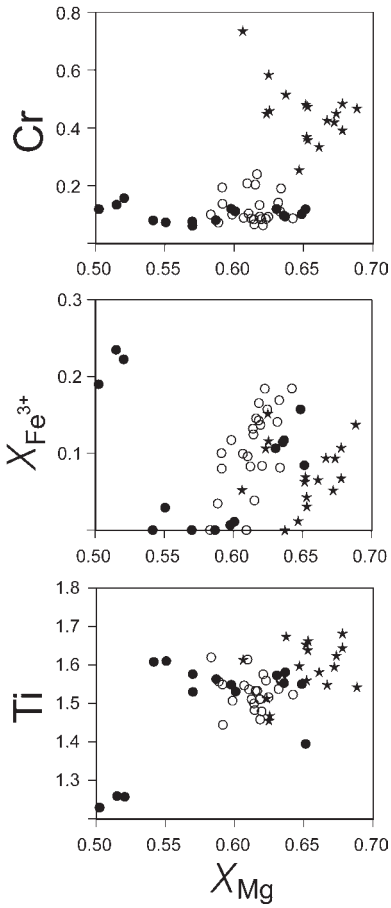

FIGURE 4. Bivariate Cr, X_{Fe}^{3+}, Ti vs. X_{Mg} diagrams showing compositional features of högbomite in association A (solid and open circles) and association B (stars) samples from the Diadina

(2002). Although different polysome types may occur at one locality (cf., Petersen et al. 1989; Visser et al. 1992), we have recast the högbomite analyses of the three samples studied based on the 2*N*3*S*-polysome formula (28 cations and 39 O atoms) because of the close resemblance with 2*N*3*S*-polysome compositions.

Compositional variation of högbomite in the studied rocks and comparison with other occurrences

The analyzed högbomite grains are unzoned and characterized by high TiO_2 contents (6.5–8.8 wt%). Some of the analyses from association B högbomite exceed most of the published TiO_2 values for this mineral in a wide range of geological conditions (Table 5). Although no distinct difference in terms of the TiO_2 contents could be noticed between the two associations, some högbomite grains in association A that are close to spinel and biotite but not in physical contact with ilmenite or rutile show the lowest TiO_2 contents (6.3–6.5 wt%). The MnO and ZnO contents of all the analyzed grains are low (<0.7 wt% and mostly below 0.3 wt%) and show no distinct difference between the two associations. Similarly the Sn concentrations are uniformly very low. The Cr_2O_3 contents, on the other hand, show a striking difference with very high values (up to 3.62 wt%) in the sapphirine-bearing association B compared to association A (<1 wt% Cr_2O_3). To the best of our knowledge, association B högbomite records the highest Cr_2O_3 values ever published (Table 5). The concentrations of NiO (0.19–0.22 and 0.46–0.50 wt% in associations A and B, respectively) mimic the results of Cr_2O_3.

The computation of the Mg-number of högbomite depends upon the choice of the recalculation scheme (Grew et al. 1987; Petersen et al. 1989; Visser et al. 1992). For this reason, many authors define $X_{Mg} = Mg/(Mg + Fe_{tot})$ without making any correction for the Fe^{+3} content (cf., Ackermand et al. 1983; Petersen et al. 1989). The X_{Mg} values of the analyzed högbomite have been computed assuming $X_{Mg} = Mg/(Mg + Fe_{tot})$ and $Mg/(Mg + Fe^{+2})$ respectively. It is evident that irrespective of the choice of the model,

TABLE 4. — *extended*

K237-37 B spr	K237-37 B spr	K237-37 B amph	K237-37 B amph	K237-37 B spl,spr	K237-37 B spr,spl
0.02	0.02	0.04	0.03	0.02	0.06
8.36	8.06	8.51	8.03	7.89	8.72
61.01	60.37	60.31	60.02	60.52	60.34
2.10	1.82	2.25	2.32	2.24	2.56
12.36	13.08	12.87	12.68	14.77	12.89
0.00	0.02	0.03	0.00	0.01	0.00
13.47	12.79	13.49	13.55	12.24	12.70
0.48	0.46	0.48	0.49	0.47	0.50
0.07	0.12	0.08	0.11	0.20	0.19
97.87	96.72	98.06	97.22	98.37	97.97
0.005	0.004	0.011	0.007	0.006	0.015
1.590	1.556	1.620	1.538	1.509	1.670
18.184	18.255	17.987	18.020	18.125	18.099
0.419	0.368	0.450	0.467	0.449	0.514
0.206	0.258	0.300	0.422	0.396	0.017
2.408	2.548	2.423	2.279	2.743	2.727
0.000	0.004	0.007	0.000	0.003	0.000
5.076	4.891	5.088	5.145	4.635	4.819
0.098	0.095	0.098	0.100	0.096	0.102
0.013	0.022	0.016	0.021	0.038	0.036
0.67	0.65	0.67	0.69	0.62	0.63
0.66	0.63	0.65	0.65	0.59	0.63
0.05	0.07	0.09	0.14	0.11	0.00

association B högbomites have distinctly higher X_{Mg} compared to those of the sapphirine-free association A. This observation supports the contention of Ackermand et al. (1983) that högbomite is more magnesian in the presence of rutile than ilmenite ± rutile. The higher concentrations of Cr, Ni, and the higher X_{Mg} values (Table 4, Fig. 4) suggest that association B rocks were derived from mafic to ultramafic protoliths. The structural formulae calculated based on 2*N*3*S*-polysome symmetry indicate high $Fe^{+3}/(Fe^{+3} + Fe^{+2})$ ratios in most of the grains (Table 4; Fig. 4). Much higher values are obtained if the procedure of Gatehouse and Gray (1982) is followed ($X_{Fe^{3+}} \geq 0.35$). The $X_{Fe^{3+}}$ values are much higher in both associations than are those of the coexisting phases such as amphibole, biotite, ilmenite, and spinel (see Tables 1–3).

Association B högbomite, like the three published sapphirine-högbomite associations (i.e., Norway: Visser et al. 1992; Greenland: Ackermand et al. 1983; Greece: Liati and Seidel 1994), is highly magnesian. However, association B högbomite is distinctly richer in Cr_2O_3 and TiO_2. A compilation of published högbomite compositions in Table 5 shows that association B högbomite has one of the highest Cr_2O_3 contents reported so far. Högbomite in sapphirine-free association A, on the other hand, differs markedly from högbomite in a similar occurrence (Aldan shield: Grew et al. 1989). In comparison to this area, the Aldan shield occurrence is distinctly more magnesian and TiO_2 rich but slightly poorer in ZnO. This difference possibly can be explained by the compositional variation and modal abundance of the minerals in the two occurrences (Table 5).

A striking feature is that högbomite compositions practically mimic the compositional changes of the associated spinel in terms of Cr_2O_3, MnO, ZnO, and X_{Mg} (see Tables 1, 4). These characteristics further corroborate the petrographic observation that högbomite grew at the expense of spinel in most domains of the two associations. Similar relations have been established from several högbomite occurrences (cf., Coolen 1981; Ackermand et al. 1983; Grew et al. 1987, 1989, 1990; Petersen et al. 1989; Visser et al. 1992; Razakamanana et al. 2000 and the references cited therein).

Chemical substitution and fractionation of elements between högbomite and the coexisting phases

Existing structural refinement studies have demonstrated that each of the spinel-like and nolanite modules are charge balanced (Hejny and Armbruster 2002). This finding implies that the entry of Ti (and/or Sn) and the required charge balance occur in the nolanite unit (Gatehouse and Gray 1982; Armbruster 1998; Hejny and Armbruster 2002). Based on site distribution data, Hejny and Armbruster (2002) postulated a substitution of the type $Ti^{4+} + R^{+2} \leftrightarrow 2R^{+3}$ in the octahedral site of the nolanite unit. A similar substitution scheme also was proposed for högbomites from several natural occurrences (Ackermand et al. 1983; Grew et al. 1990; Visser et al. 1992; Razakamanana et al. 2000). Despite their rather limited compositional variation, the studied högbomites show a strong negative correlation between $Ti + R^{+2}$ and $2R^{+3}$ and a positive correlation for Ti and R^{+2} (Fig. 5), which supports the substitution scheme postulated by these workers. The good negative correlation between Fe^{+3} and Al + Cr indicates a substitution between these elements (Fig. 5). This corroborates the observation of Hejny and Armbruster (2002) that in the T_1 layer, the cation distribution in the T site is dependent on the Ti content of the octahedron.

Although a compositional gap exists, the Fe-Mg partitioning between högbomite and coexisting spinel shows a remarkable linear trend (with $R^2 > 0.9$), irrespective of the choice of the valence state of Fe (Fig. 6). Existing Fe-Mg partitioning data show diverse patterns but in most cases, (Fe_{tot}/Mg) högbomite ≥ (Fe/Mg) spinel (Coolen 1981; Petersen et al. 1989), similar to our data. However, after correction for Fe^{+3} based on the 2*N*3*S* structural formula, most of the högbomite grains appear to be distinctly more magnesian compared to the coexisting spinel $\{K_D [(Fe^{2+}/Mg)^{Hög}/(Fe^{2+}/Mg)^{Spl} = 0.59–0.91]\}$.

Published högbomite analyses all show insufficient Al to fill up the R^{+3} sites irrespective of the polysome assumed, indicating substantial substitution of Fe^{3+}. This result is further supported by the existing structure refinement data (cf., Gatehouse and Gray 1982; Grew et al. 1987; Petersen et al. 1989; Hejny and Armbruster 2002 and references cited therein). Experimental data in the systems Fe_3O_4-$FeAl_2O_4$-$MgAl_2O_4$, on the other hand, demonstrate a very limited proportion of Fe^{+3} in the structure of spinel at temperature ≤650 °C (less than 10 mol% Fe_3O_4 in spinel and <5 mol% Fe_2O_3 in ilmenite, cf., Sack and Ghiorso 1991). This finding is supported by the low values of Fe^{+3} in these two minerals in low- to medium-grade rocks. Ilmenite can accommodate significant Fe^{+3} in this temperature range (up to 30 mol% Fe_2O_3; cf., Burton 1991). However, at low f_{O_2}, when this mineral coexists with rutile in the absence of magnetite, the solubility of Fe^{+3} is strongly reduced (discussed in Spear 1993). This conclusion is corroborated by the ilmenite analyses from the studied rocks as well as from several other högbomite occurrences (see Table 5).

Combining the crystallographic, experimental, and phase-compositional data, it can be stated that högbomite will be a major sink of Fe^{+3} in metamorphic rocks (particularly those with rutile + ilmenite but devoid of magnetite) under greenschist- and

TABLE 5. The polysome type and some important compositional characteristics of högbomite from well studied occurrences

Area/Reference	Important phases with högbomite	Composition of högbomite	Högbomite polytype assumed/ determined *(metamorphic conditions)*
Greenland Ackermand et al. 1983	spr, chl, ged, ath, hbl, spl, rt	TiO_2 = 5.7–8.1 Cr = 0.05–0.11 Zn = 0.09–0.15, CrSpl = 0.05–0.09 Fe^{+2}/Fe^{+3} nd	8*H*(?), structural formulae on 31oxygens (~ 500 °C, P unknown)
Norway Visser et al. 1992	spr, ilm, mag, crn, spl, crd, rt, ged	TiO_2 = 9.55; 5.66 Cr = 0.24; 0.05 Zn = l CrSpl = ~0.02 Fe^{+2}/Fe^{+3} = 0.53; 0.77	8*H*, 10*H*(?) *(550-620 °C, 6-7 kbar)*
S. Australia Teale,1980 Hejny & Armbruster 2002	spl, bt, rt, crn	TiO_2 = 3.9–5.19 Cr = nd Zn = 0.19–0.53 CrSpl nd Fe^{+2}/Fe^{+3} = 1.15	10*T* *(Amphibolite facies)*
Tamil Nadu, India Grew et al. 1987	krn, sil, rut, crd, chl, spl, mag	TiO_2 = 2.49–2.47 Cr = 0.71–0.82 Zn = 0.98–1.04, CrSpl =1.68–3.22 Fe^{+2}/Fe^{+3} = 0.90–1.05	8*H* *(680-720 °C, 6.5 kbar)*
Aldan shield Grew et al. 1989	spl, mt, crn, pl, bt, czo, ms, rt(?)	TiO_2 = 5.3–5.55 Cr = 0.17–0.2 CrSpl = ~0.1 Fe^{+2}/Fe^{+3} = 1.89–2.15	8*H* *(Amphibolite facies)*
Benson mines, USA Petersen et al. 1989	spl, crn, qtz, sill, grt, bt, ilm, rt	TiO_2 = 4.44–5.42 Cr = ~0.00 Zn = 2.44; 3.22 CrSpl nd Fe^{+2}/Fe^{+3} nd	8*H* *(730 °C, 7.5 kbar)*
Manitouwadge,Canada Petersen et al. 1989	ged, crd, st, spl, mt, ilm, rt, bt	TiO_2 = 1.86–5.48 Cr = 0.00–0.07 Zn = 8.13–17.53 CrSpl = 0.01; 0.15 Fe^{+2}/Fe^{+3} nd	8*H*/10*H* *(650 °C,6 kbar)*
Madagaskar Razakamana et al. 2000	spl, ilm, crn, crd, chl, rt	TiO_2 = 5.51–7.12 Cr = 0.15–0.62 Zn = 0.23; 0.91 CrSpl = 0.13–0.60 Fe^{+2}/Fe^{+3} = 0.31–1.6	8*H* *(700±100 °C, 6±1 kbar)*
N. Greece Liati & Seidel 1994	ky, rt, pl, spl, spr, crn, omp	TiO_2 = 6.42; 5.85 Cr = 0.28; 0.15 Zn nd CrSpl nd Fe^{+2}/Fe^{+3} = 1.19; 1.32	8*H* *(700 °C, 10-15 kbar)*
Sweden, Spain, Tanzania Coolen 1981	Högbomite in Fe-Ti ores in Sweden and Tanzania, metaperidotite in Spain	TiO_2 = 4.81–8.11 Cr = 0.00–2.08 Zn nd CrSpl = 0.00–1.32 Fe^{+2}/Fe^{+3} = 0.23–85	10*H*(?), structural formulae on 8 oxygens and R^{+3} = 4 *(700-750 °C, 6-10 kbar)*
Tanzania, Zakrzweski 1977 Hejny & Armbruster 2002	Högbomite in Fe-Ti ores	TiO_2 = 6.42–10.44 Cr = 0.31–1.22 Zn = 0.36–0.92 CrSpl nd Fe^{+2}/Fe^{+3} = 0.47–1.36	24*R* *(Garnet grade)*
East Antarctica Grew et al. 1990	qtz, grt, sill, crd, spl, rt, crn, krn	TiO_2 = 4.45–7.41 Cr = 0.00–0.09 Zn = 2.74–8.92 CrSpl = 0.00–0.12 Fe^{+2}/Fe^{+3} nd	8*H* *(≤ 500 °C, ~2 kbar)*
S.Africa Beukes et al. 1986	crd, ged, bt, hbl, chl, cpx	TiO_2 = 3.76–5.82 Cr = 0.01–0.23 Zn = 0.49–4.05 CrSpl = 0.01–0.14 Fe^{+2}/Fe^{+3} = 3.44–7.5	4*H*, 5*H* *(Upper amphibolite facies)*

Note: CrSpl = wt% Cr_2O_3 in the coexisting spinel. nd = not analyzed/detected. Polysome types according to the authors.

amphibolite-facies conditions. As a result, Mg will be preferentially fractionated into högbomite compared to the coexisting spinel under greenschist- and amphibolite-facies conditions over a range of oxidation states lying above the magnetite-wüstite buffer (cf., Coolen 1981; Grew et al. 1987, 1989, 1990; Visser et al. 1992; Liati and Seidel 1994; Razakamanana et al. 2000). Due to the low ZnO contents in most of the analyzed högbomite and spinel grains, the nature of fractionation of these elements could only be calculated for six pairs (see Fig. 6). The Zn/Fe^{+2} ratios define a perfect linear trend with K_D^{Spl} ranging between 0.47 and 0.88. Similarly, the Fe^{2+}-Mg distribution between högbomite and coexisting garnet shows a linear trend $\{K_D\ [(Fe^{2+}/Mg)^{Grt}/(Fe^{2+}/$

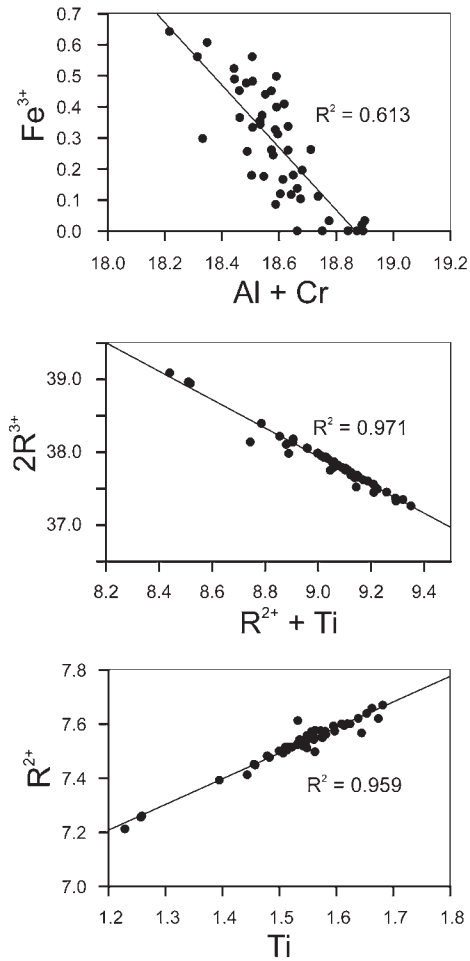

FIGURE 5. Bivariate plots showing the important substitutional trends in högbomite from the Diadina occurrence.

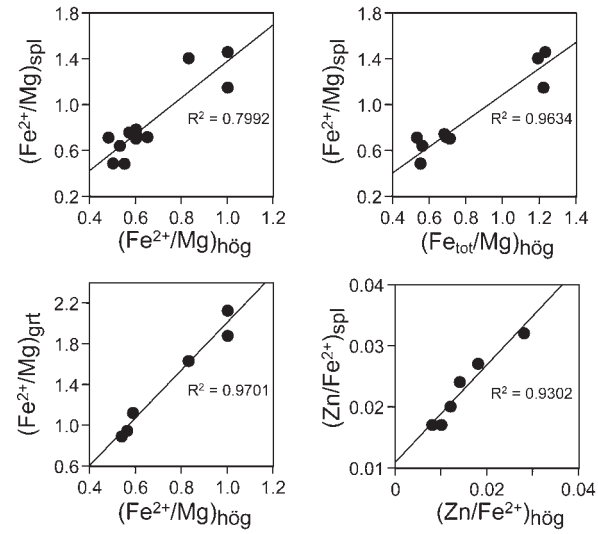

FIGURE 6. Bivariate plots illustrating the distribution of Fe^{2+}, Fetot, Mg, and Zn between högbomite-spinel and h?mite-garnet pairs in samples from the Diadina occurrence.

$Mg)^{Hög}$ = 1.65–2.12]} (Fig. 6).

The Fe^{+2}-Mg distribution coefficients between högbomite and sapphirine fall in a narrow range of 4.7–5.38. High K_D values also have been reported from Greece (2.89, Liati and Seidel 1994) and Norway (3.15–3.6, Visser et al. 1992; if the Fe^{+3} recalculation for their anhydrous sample PT160 is done on the basis of 2*N*3*S* polytype as suggested by the authors). The higher K_D values for the studied samples can be explained by lower *P-T* conditions of this area compared to the other occurrences (discussed later). The mineral pairs from Greenland (Ackermand et al. 1983), however, show an erratic cation distribution and some of the högbomite analyses give $Fe_{tot} = Fe^{+3}$ when recalculated on the basis of 2*N*3*S* polytype. The highly scattered K_D data for the Greenland samples cannot be explained at the present time. Uncertainties associated with the recalculation schemes, identification of högbomite polytype, and the lack of equilibrium between these two minerals (as revealed from the petrographic descriptions) could contribute to the observed fractionation pattern.

The coefficients for Fe^{+2}-Mg partitioning between högbomite and the other coexisting ferromagnesian phases also show very restricted values [e.g., K_D(Hög-Ged) ~ 2.08–2.79; K_D(Hög-Hbl) ~ 1.62–2.31; K_D(Hög-Bt) ~ 3.46–3.84].

In conclusion, the systematic partition of Fe^{+2}, Mg, and Zn between högbomite and the coexisting minerals with narrow ranges of K_D values, suggests that högbomite was in chemical equilibrium with the associated aluminous phases.

DEVELOPMENT OF THE HÖGBOMITE ASSEMBLAGES

The textural relations and the compositional characteristics of the phases described above put important constraints on the genesis of högbomite in the studied rocks. In association A, the Mg-numbers [Mg/(Mg + Fe^{+2})] of the phases decrease in the following sequence: dolomite ≥ biotite > cordierite > calcic-amphibole > chlorite > högbomite > spinel ≥ garnet > ilmenite. This, together with the textural relations and the alumina content of the minerals, indicates the following högbomite-forming reaction:

$$\text{corundum + rutile + ilmenite + plagioclase + } Mg^{2+} + Ca^{2+} + K^{+} + H_2O + O_2 \rightarrow \text{calcic-amphibole + högbomite + biotite} \quad (1)$$

This reaction explains the development of coarse calcic-amphibole + magnesian högbomite + biotite intergrowths after corundum and the widespread inclusions of rutile and ilmenite in högbomite. The textural relations and the sympathetic variation of Cr_2O_3 and ZnO in the product högbomite and the coexisting spinel suggest that spinel was also a reactant phase, at least in some domains.

The high Fe^{+3}/Fe^{+2} ratio in högbomite and its low values in the reactant phases indicate that the infiltrating fluid was oxidizing and hence oxygen was a reactant. Similar oxidation and hydration reactions for the genesis of högbomite have been reported from several occurrences (cf., Ackermand et al. 1983; Grew et al. 1987, 1990; Petersen et al. 1989; Razakamanana et al. 2000 among others).

The textural features such as rimming of rutile by ilmenite close to högbomite in spinel-bearing domains and development

of högbomite at the junctions of corundum and ilmenite suggest the operation of the following redox reactions involving only the oxide minerals:

$$\text{spinel} + \text{rutile} + H_2O + O_2 \rightarrow \text{högbomite}_{ss} + \text{ilmenite} \quad (2a)$$

$$\text{corundum} + \text{ilmenite} + H_2O + O_2 \rightarrow \text{högbomite} + \text{rutile} \quad (2b)$$

The presence of abundant calcic-amphibole and lack of any primary calcic and magnesian phases in most domains are intriguing. Although it is not possible to estimate the composition and the abundance of these phases prior to the formation of calcic-amphibole + högbomite, the observed textural and compositional data cannot completely rule out the possibility of some Ca- and Mg-metasomatism during the operation of the hydration reaction 1.

Garnet-chlorite-dolomite developed after calcic-amphibole by the reaction:

$$\text{calcic-amphibole} + \text{corundum} + Na^+ + CO_2 + H_2O \rightarrow \text{garnet} + \text{chlorite} + \text{plagioclase} + \text{dolomite} + \text{calcite} \quad (3)$$

Reaction 3 can explain the textural relations and the compositional attributes discussed earlier.

In association B, the Mg-number of the ferromagnesian phases increases in the following sequence: ilmenite < spinel < högbomite ≤ chlorite < gedrite ≤ calcic amphibole < sapphirine < magnesite. The textural relations such as sapphirine+gedrite+ högbomite intergrowths replacing calcic-amphibole, and spinel developing at the contact of calcite can be explained by the reaction:

$$\text{calcic-amphibole} + \text{spinel} + \text{rutile} + H_2O + CO_2 + O_2 \rightarrow \text{gedrite} + \text{sapphirine} + \text{högbomite} + \text{calcite} \quad (4)$$

In view of the Fe-Mg partitioning data among the phases, reaction 4 only can be balanced if Mg is a reactant. The presence of magnesite in many of the sapphirine-högbomite domains indicates that either MgO was added to the system by the metamorphic fluid during reaction 4, or the carbonate phase was stabilized early and reacted during the formation of the sapphirine + högbomite intergrowth. In the chlorite-present domains, the following reaction could also operate in the absence of calcic-amphibole:

$$\text{spinel} + \text{gedrite} + \text{magnesite} + \text{rutile} + H_2O + O_2 \rightarrow \text{sapphirine} + \text{högbomite} + \text{chlorite} + CO_2 \quad (5)$$

Reactions 4 and 5 possibly operated together in some domains and explain the presence of chlorite in many högbomite-sapphirine intergrowths. However, as in reaction 4, it is also possible that the additional MgO required for the formation of the assemblage sapphirine + chlorite + högbomite was provided by the metamorphic fluid, and magnesite also was produced during Mg metasomatism. Replacement of gedrite-sapphirine by chlorite in some högbomite-free domains tends to support Mg metasomatism during and subsequent to högbomite formation at least in some areas:

$$\text{gedrite} + \text{sapphirine} + Mg^{+2} + CO_2 + H_2O \rightarrow \text{chlorite} + \text{magnesite} \quad (6)$$

Physical conditions of högbomite formation

It has been demonstrated above that högbomite in the studied rocks developed during amphibolite-facies metamorphism/metasomatism. Therefore, the mineralogy and the compositional attributes of the studied suite of rocks can be used to constrain the *P-T* conditions of metamorphism and, hence, of högbomite formation.

The stability of the assemblage garnet + cordierite + corundum ± spinel in association A provides an upper limit on the metamorphic pressure. This assemblage is bivariant in the system FMAS and is stable at pressures that are below those defined by the related univariant equilibria garnet + Al_2SiO_5 ↔ spinel + cordierite + corundum (cf., Sengupta et al. 1999). The FMAS univariant reaction has a flat slope in *P-T* space and passes through ~7 kbar and ~840 °C (see Sengupta et al. 1999). It follows that under amphibolite-facies conditions, the maximum pressure that is permissible to prevent the appearance of aluminosilicate will be below 7 kbar.

The common occurrence of the assemblages staurolite + anthophyllite ± gedrite, garnet + staurolite + calcic-amphibole, and kyanite + calcic-amphibole + biotite + plagioclase in the closely associated högbomite-free rocks puts additional constraints on the *P-T* conditions. Because the compositions of these phases (other than the calcic-amphibole) can be approximated in the system FeO-MgO-Al_2O_3-SiO_2, the petrogenetic grid developed by Spear and Rumble (1986) is expected to delimit their stability fields. In Figure 7, a part of the petrogenetic grid relevant to the observed assemblages has been reproduced. It is evident from the figure that the stability of the assemblages gedrite + staurolite + anthophyllite (instead of gedrite + cummingtonite or staurolite+orthoamphibole-bearing assemblages) and garnet + cordierite + corundum ± spinel (instead of Al_2SiO_5-bearing assemblages) tightly constrains the *P-T* conditions at 6 ± 1 kbar and 540 to ~630 °C. The predicted temperatures are corroborated by independent temperature estimates obtained from garnet-amphibole (Graham and Powell 1984), garnet-biotite (Pigage and Greenwood 1982), and garnet-chlorite (Dickenson and Hewitt 1986) thermometry (500–600 °C). The estimated temperature is also consistent with the low TiO_2 content of the calcic-amphibole equilibrated with Ti-saturating phases such as rutile, ilmenite, and högbomite (<0.9 wt%, Raase et al. 1986; Ernst and Liou 1998). Garnet-cordierite Fe^{2+}-Mg exchange thermometry (Bhattacharya et al. 1988), on the other hand, yields significantly higher temperature estimates (730–760 °C) that are inconsistent with the stability of staurolite and kyanite (instead of sillimanite at the estimated pressure) in the associated rocks, and the low Ti-content of amphibole. The garnet-cordierite thermometer is calibrated for granulite-facies conditions, and is not expected to provide reasonable temperature estimates for low-grade rocks because of the large extrapolation from the *P-T* conditions of calibration. The lower stability limit of sapphirine in the system MgO-Al_2O_3-SiO_2-H_2O is defined by the reaction sapphirine +

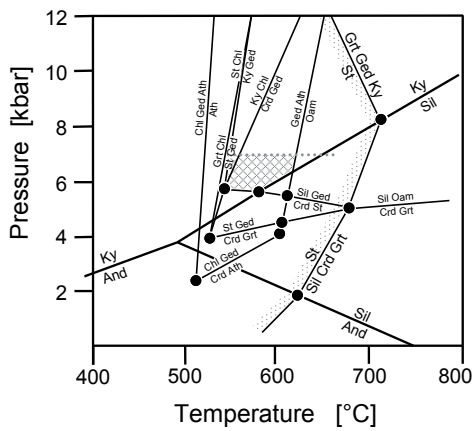

FIGURE 7. Partial petrogenetic grid for the system FeO-MgO-Al_2O_3-SiO_2 showing reactions that are relevant to the assemblages of the studied blackwall samples from the Diadina occurrence. (adopted from Spear and Rumble 1986). The cross-hatched field indicates the stability field of the högbomite-bearing assemblages.

H_2O ↔ corundum + chlorite + spinel. This reaction is nearly pressure insensitive and is placed at ~700 °C in the pure MASH system (Seifert 1974). Considering the significant contents of Fe^{+3} and Fe^{+2} components in the studied sapphirine (see Table 2), and the presence of a mixed fluid, the reaction is expected to be displaced to lower temperature by more than 100 °C making the sapphirine stable in the *P-T* window estimated above. Similar conclusions were also drawn for a sapphirine + högbomite association from Greenland (Ackermand et al. 1983).

DISCUSSION

It is evident from the foregoing analysis that the diverse högbomite-bearing assemblages in the studied area were developed in different compositional domains under nearly isothermal isobaric conditions. Like other occurrences, högbomite grains in the studied rocks grew over spinel and mimic the composition of the latter mineral (cf., Grew et al. 1990). However, our petrological data do not support a formation of högbomite through "oxidation-exsolution" of a homogeneous Ti-spinel or Ti-Al magnetite, as has been advocated in many areas (Petersen et al. 1989; Grew et al. 1990; Razakamanana et al. 2000). Instead, the formation of this mineral can be explained best by complex mineral-fluid equilibria involving several oxide-silicate and carbonate phases. The petrological attributes indicate growth of this mineral during the peak conditions of regional amphibolite-facies metamorphism/metasomatism. In this respect, the studied rocks contrast with many other occurrences where the formation of högbomite has been linked with retrogressive metamorphism and hydration (reviewed in Grew et al. 1990). The compositional attributes of högbomite in the studied samples are consistent with the 2*N*3*S*-polysome, which is substantiated by crystallographic data for association B högbomite. The systematic Fe^{+2}-Mg distribution data for högbomite and the associated phases (such as spinel, sapphirine, and garnet) suggest attainment of chemical equilibrium. Geothermobarometry together with the constraints imposed by the phase equilibria tightly bracket the *P-T* conditions at 6 ± 1 kbar and 600 ± 50 °C. The estimated temperature value overlaps with the estimates from most of the other högbomite occurrences and only a few areas record higher temperatures (see Table 5). Although the metamorphic fluid compositions could not be measured directly, the presence of both hydrate and carbonate phases in both associations indicate involvement of a mixed CO_2-H_2O fluid.

Högbomite in the studied area, as in other occurrences, shows significant Fe^{+3} contents and commonly develops on minerals with lower Fe^{+3}/Fe^{+2} ratios. This observation, together with the intimate relations of this mineral with a variety of Fe-Ti-Al oxides, sulfides, and carbonate phases in the different occurrences, points to a strong influence of the ambient fluid compositions on the stability of the högbomite-bearing assemblages (in addition to pressure and temperature). The control of fluid composition on högbomite equilibria can be depicted in the simple system FeO-Al_2O_3-TiO_2-O_2-S_2-H_2O. Petersen et al. (1989) studied the phase relations of some högbomite-bearing assemblages in an isothermal–isobaric log f_{O_2}-log f_{S_2} plane of the stated system. The derived phase diagram provides valuable insights into the role of fluid composition on the stability of many högbomite-bearing assemblages. However, a modification of their log f_{O_2}-log f_{S_2} diagram is required for several reasons. First, Petersen et al. (1989) considered magnetite to be present in the entire range of log f_{O_2}-log f_{S_2} window, and rutile to be present only at f_{O_2} higher than those defined by the reaction ilmenite + O_2 ↔ rutile + magnetite. Rumble (1976) showed that at f_{O_2} values lower than defined by this redox reaction, either ilmenite+magnetite or rutile+ilmenite will be stable depending upon the Fe/(Fe + Ti) ratio of the rock. It follows that in rocks having low Fe/(Fe + Ti) ratios, the högbomite-forming reactions will involve ilmenite + rutile instead of ilmenite + magnetite at low f_{O_2}. This conclusion is supported by the petrological features of the studied rocks and also of other magnetite-free högbomite occurrences. Second, petrographic observations in the majority of reported occurrences document the involvement of spinel in most of the högbomite-forming reactions (reviewed in Grew et al. 1990; Razakamanana et al. 2000). Yet, this phase is not considered in the study of Petersen et al. (1989). Third, in some occurrences högbomite is found to have grown over the sulfide minerals (cf., Fig. 1E of Petersen et al. 1989). This feature requires consideration of the relevant sulfide-högbomite equilibria.

In view of this, we have developed a partial isothermal-isobaric log f_{O_2}-log f_{S_2} topology in the system FeO-Al_2O_3-TiO_2-O_2-S_2-H_2O at constant f_{H_2O}, involving the phases högbomite, ilmenite, corundum, magnetite, rutile, pyrite, pyrrhotite, hercynite, and fluid. To interpret the textural features of the studied rocks (and also in other rutile-saturated rocks), we have considered the mineral reactions around the isothermal-isobaric invariant points [Spl] and [Crn]. Although rutile is omnipresent in the studied rocks, the two rutile-absent reactions are also shown to complete the topology. The latter reactions will also help to explain the reactions in rocks with low Fe/(Fe + Ti) ratios. The isothermal-isobaric univariant reactions around the invariant points [Spl] and [Crn] are presented in the Table 6. In calculating the mineral reactions, the högbomite composition has been assumed to be $Fe_5R^{3}_{16}TiO_{30}(OH)_2$ following the procedure of Petersen et al. (1989). However, recalculation of the structural formulae based on other polysome types will not change the overall phase relations. In computing the coefficients of the phases in each reaction,

the variable Fe^{+2}/Fe^{+3} ratios of högbomite have been considered (see Table 6). Although this ratio also changes in the ilmenite, its composition has been taken to be pure $FeTiO_3$ as it always coexists with rutile and has low Fe^{+3} contents in the studied rocks. The slopes of the isothermal-isobaric univariant reactions have been computed using the relations $d(\log f_{O_2})/d(\log f_{S_2}) = -n1/n2$, where $n1$ and $n2$ are the coefficients of S_2 and O_2 respectively in a balanced reaction. Because the Fe^{+3} content of högbomite increases with increasing f_{O_2}, some of the univariant reactions will change their slope with increasing oxidation state.

The arrangements of the univariant reactions around the isothermal-isobaric invariant points [Spl] and [Crn] have been computed following the Schreinemakers principles (Fig. 8). Several interesting features emerge from the reaction topology of the $\log f_{O_2}$-$\log f_{S_2}$ diagram. The most striking features include: (1) The stability of the högbomite-bearing assemblages is restricted to a narrow field bounded by redox and oxide-sulfide equilibria. At lower f_{O_2} and f_{S_2}, högbomite is stabilized from spinel, corundum, and one of the Ti-saturating phases (rutile or ilmenite) with increasing f_{O_2}. The bivariant redox reactions explain the growth of högbomite (with significant Fe^{+3}) at the expense of ilmenite+corundum (both having low Fe^{+3}) and spinel+rutile in association A (discussed earlier) and in many other reported högbomite occurrences (cf., Grew et al. 1990, Petersen et al. 1989). These reactions also explain the formation of högbomite granules during concomitant hydration and "oxidation-exsolution" of a spinel and/or magnetite solid solution (Petersen et al. 1990; Grew et al. 1990). The topological constraints of the Figure 8 suggest that högbomite will appear at lower f_{O_2} in Ti-rich rocks compared to the Ti-poor magnetite-bearing assemblage. (2) With increasing f_{O_2}, the stability of högbomite will initially increase as it can accommodate a large amount of Fe^{+3}. However, after reaching some critical f_{O_2} value, the mineral will break down to the more-oxidized assemblage corundum + magnetite + rutile. This result explains the absence of högbomite in the assemblage hematite+rutile but its common occurrence with magnetite, Ti-rich hematite, and ferrian ilmenite (Table 5). The $\log f_{O_2}$-$\log f_{S_2}$ topology, therefore, indicates that the stability of högbomite in natural systems will be restricted to a narrow f_{O_2} window defined by the assemblages högbomite + ilmenite + rutile ± spinel ± corundum and högbomite + magnetite + rutile+corundum (see Fig. 8). Grew et al. (1990) also inferred a similar situation for the stability of natural högbomite. (3) High f_{S_2} severely reduces the stability of högbomite, and sulfides + Fe-Ti-Al oxides forms instead (see Fig. 8). Increasing temperature and the presence of a mixed CO_2-H_2O fluid has similar inhibiting effects (see the displacement of the invariant points and the related univariant equilibria in Fig. 8). Mg-rich bulk compositions, on the other hand, will enlarge the högbomite stability field, as this element is preferentially partitioned into högbomite.

It is evident from the foregoing discussion that distinct physico-chemical conditions are needed for the formation of the högbomite. This explains the rarity of this mineral although its chemical ingredients are common in natural systems (also discussed in Grew et al. 1990). The available petrological data and the topological constraints of Figure 8 suggest that metamor-

TABLE 6. Some balanced univariant and bivariant reactions around the isothermal-isobaric invariant points [Hc] and [Crn] in the system Fe-Al-Ti-O-H-S

[Hc]

Univariant reactions

(Ilm): $(8 + y)Py/Po + Rt + (8 - 0.5y)Crn + 0.5(9 + 1.5y)O_2 + H_2O \leftrightarrow Fe_5Al_{(16-y)}Fe^{+3}_yTiO_{30}(OH)_2 + Mt + (8 + y)S_2/S$

(Rt): $(7 + y)Py/Po + (8 - 0.5y)Crn + Ilm + 0.5(8 + 1.5y)O_2 + H_2O \leftrightarrow Mt + Fe_5Al_{(16-y)}Fe^{+3}_yTiO_{30}(OH)_2 + (7+y)S_2/S$

(mt): $(6 + y)Py/Po + 2Rt + (8 - 0.5y)Crn + 0.5(6 + 1.5y)O_2 + H_2O \leftrightarrow Fe_5Al_{(16-y)}Fe^{+3}_yTiO_{30}(OH)_2 + Ilm + (6 + y)S_2/S$

(Py/Po,Hög): $3\,Ilm + 0.5O_2 \leftrightarrow 3\,Rt + Mt$

Bivariant reactions

$(5 + y)Ilm + (8 - 0.5y)\,Crn + 0.25y\,O_2 + H_2O \leftrightarrow Fe_5Al_{(16-y)}Fe^{+3}_yTiO_{30}(OH)_2 + (4 + y)Rt$

$Fe_5Al_{(16-y)}Fe^{+3}_yTiO_{30}(OH)_2 + 0.5(1.66 - .16y)O_2 + H_2O \leftrightarrow (8 - 0.5y)Crn + Rt + 0.333(5 + y)Mt$

[Crn]

Univariant reactions

(Ilm): $(8 - 0.5y)Hc + Rt + Py/Po + 1.165O_2 + H_2O \leftrightarrow Fe_5Al_{(16-y)}Fe^{+3}_yTiO_{30}(OH)_2 + 0.333(4 - 1.5y)Mt + S_2/S$

(Rt): $(8 - .5y)Hc + Ilm + Py/Po + 1.34O_2 + H_2O \leftrightarrow Fe_5Al_{(16-y)}Fe^{+3}_yTiO_{30}(OH)_2 + 0.333(5 - 1.5y)Mt + S_2/S$

(Mt): $(8 - 0.5y)Hc + Py/Po + (5 - 1.5y)Rt + 0.5(0.5y - 1)O_2 + H_2O \leftrightarrow Fe_5Al_{(16-y)}Fe^{+3}_yTiO_{30}(OH)_2 + (4 - 1.5y)Ilm + S_2/S$

(Hc,Py/Po): $3Ilm + 0.5O_2 \leftrightarrow 3Rt + Mt$

Bivariant reactions

$(8 - 0.5y)Hc + (4 - 1.5y)Rt + 0.25O_2 + H_2O \leftrightarrow Fe_5Al_{(16-y)}Fe^{+3}_yTiO_{30}(OH)_2 + (3 - 1.5y)Ilm$

$(8 - 0.5y)Hc + Rt + H_2O + 0.5\,O_2 \leftrightarrow Fe_5Al_{(16-y)}Fe^{+3}_yTiO_{30}(OH)_2 + 0.333(1.5y - 3)\,Mt$

$(8 - 0.5y)Hc + Ilm + 0.67O_2 + H_2O \leftrightarrow Fe_5Al_{(16-y)}Fe^{+3}_yTiO_{30}(OH)_2 + 0.333(4 - 1.5y)Mt$

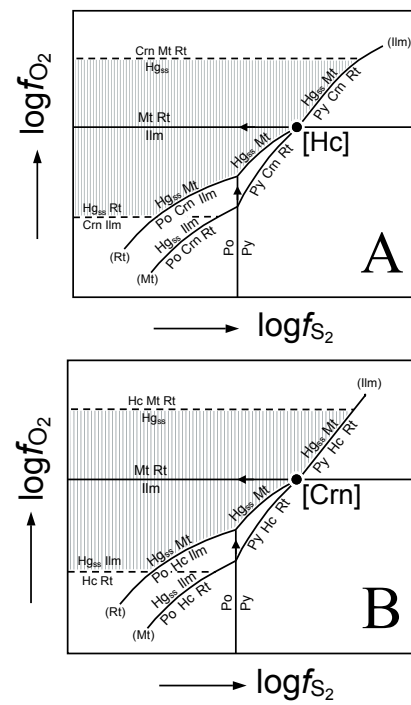

FIGURE 8. Isothermal-isobaric $\log f_{O_2}$-$\log f_{S_2}$ diagrams in parts of the system Fe-Al-Ti-O-S-H illustrating the reactions topologies around the invariant point [Hc] (A) and the invariant point [Crn] (B). The dashed lines indicate the bivariant reactions. The lined field marks the stability of the högbomite-bearing assemblages at the Diadina occurrence. Arrow heads indicate the directions of displacement of the reactions due to a reduced a_{H_2O}. The slopes of some of the reactions are curved because they change as a function of the change of Fe^{+2}/Fe^{+3} in högbomite (see text).

phism of titanian and aluminous protoliths under greenschist- to amphibolite-facies conditions will be most suitable for the growth of högbomite if f_{H_2O} is high, f_{S_2} low, and the oxidation states do not depart much from those defined by the paragenesis ilmenite$_{ss}$ + rutile + magnetite.

ACKNOWLEDGMENTS

P.S. acknowledges the Alexander von Humboldt Stiftung, Germany, for a research fellowship during which this work was carried out. Field work of M.R. in Russia has been funded by the Deutsche Forschungsgemeinschaft (DFG). We thank Beate Spiering for the help with the electron microprobe work. Careful reviews by T. Armbruster, E.U. Petersen, D. Visser, and editorial comments by J. Thomson were very helpful.

REFERENCES CITED

Ackermand, D., Windley, B.F., and Herd, R.K. (1983) Magnesian högbomite in a sapphirine-bearing rock from the Fiskenaesset region, W. Greenland. Mineralogical Magazine, 47, 557–561.

Armbruster, T. (1998) Zincohögbomite-8H from Samos (Greece): crystal structure, polysomatism, and polytypism in högbomite related structures. Schweizerische Mineralogische und Petrographische Mitteilungen, 78, 461–468.

———(2002) Revised nomenclature of högbomite, nigerite, and taaffeite minerals. European Journal of Mineralogy, 14, 389–395.

Beukes, G.J., van Zyl, V.C., Schoch, A.E., DeBruiyn, H., van Aswegen, G., and Strydom, D. (1986) A högbomite-spinel-gedrite-paragenesis from northern Bushmanland, Namaqua mobile belt, South Africa. Neues Jahrbuch für Mineralogie Abhandlungen, 155, 53–66.

Bhattacharya, A., Mazumdar, A.C., and Sen, S.K. (1988) Fe-Mg mixing in cordierite: Constraints from natural data and implications for cordierite-garnet geothermometry in granulites. American Mineralogist, 73, 338–344.

Bibikova, E., Skiöld, T., Bogdanova, S., Gorbatschev, R., and Slabunov, A. (2001) Titanite-rutile thermochronometry across the boundary between the Archaean craton in Karelia and the Belomorian mobile belt, eastern Baltic Shield. Precambrian Research, 105, 315–330.

Bogdanova, S.V. and Bibikova, E.V. (1993) The "Saamina" of the Belomorian Belt: new geochronological constraints. Precambrian Research, 64, 131–152.

Burton, B.P. (1991) The interplay of chemical and magnetic ordering. American Mineralogical Society, Reviews in Mineralogy, Vol. 25, 303–322.

Coolen, J.J.M.M.M. (1981) Högbomite and aluminium spinel from some metamorphic rocks and Fe-Ti ores. Neues Jahrbuch Mineralogische Monatshefte (1981), 374–384.

Dickenson, M.P. and Hewitt, D. (1986) A garnet-chlorite geothermometer. Geological Society of America, Abstracts 18, 584.

Ernst, W.G. and Liou, J. (1998) Experimental phase-equilibrium study of Al- and Ti-contents of calcic amphibole in MORB- a semiquantitative thermobarometer. American Mineralogist, 83, 952–969.

Gaál, G. and Gorbatschev, R. (1987) An outline of the Precambrian evolution of the Baltic Shield. Precambrian Research, 35, 15–52.

Gatehouse, B.M. and Gray, I.E. (1982) The crystal structure of högbomite-8H. American Mineralogist, 67, 373–380.

Gorbatschev, R. and Bogdanova, S.V. (1993) Frontiers in the Baltic Shield. Precambrian Research, 64, 3–21.

Graham, C.M. and Powell, R. (1984) A garnet-hornblende geothermometer: calibration, testing and application to the Pelona Schist, Southern California. Journal of Metamorphic Geology, 2, 13–21.

Grew, E.S., Abraham, K., and Medenbach, O. (1987) Ti-poor högbomite in kornerupine-cordierite-sillimanite rocks from Ellammankovilpatti, Tamil Nadu, India. Contributions to Mineralogy and Petrology, 95, 21–31.

Grew, E.S., Drugova, G.M., and Leskova, N.V. (1989) Högbomite from the Aldan Shield, Eastern Siberia, USSR. Mineralogical Magazine, 53, 376–379.

Grew, E.S., Hiroi, Y., and Shiraishi, K., (1990) Högbomite from the Prince Olav Coast, East Antarctica: An example of oxidation-exsolution of a complex magnetite solid solution? American Mineralogist, 75, 589–600.

Hejny, C. and Armbruster, J. (2002) Polysomatism in högbomite: the crystal structures of 10T, 12H, 14T, and 24R polysomes. American Mineralogists, 87, 277–292.

Leake, B.E., Wooley, A.R., Arps, C.E.S., Birch, W.D., Gilbert, M.C., Grice, J.D., Hawthorne, F.C., Kato, A., Kisch, H., Krivovichev, V.G., Linthout, K., Laird, J., Mandarino, J.A., Maresch, W.V., Nickel, E.H., Rock, N.M.S., Schumacher, J.C., Smith, D.C., Stephenson, N.C.N., Ungaretti, L., Whittaker, E.J.W., and Youzhi, G. (1997) Nomenclature of amphiboles: report of the Subcommittee on Amphiboles of the International Mineralogical Association, Commission on New Minerals and Mineral Names. American Mineralogist, 82, 1019–1037.

Liati, A. and Seidel, E. (1994) Sapphirine and högbomite in overprinted kyanite-eclogites of central Rhodope, N. Greece: first evidence of granulite-facies metamorphism. European Journal of Mineralogy, 6, 733–738.

Petersen, E.U., Essene, E.J., Peacor, D.R., and Marcotty, L.A. (1989) The occurrence of högbomite in high-grade metamorphic rocks. Contributions to Mineralogy and Petrology, 101, 350–360.

Pigage, L.C. and Greenwood, H.J. (1982) Internally consistent estimates of pressure and temperature; the staurolite problem. American Journal of Science, 282, 943–969.

Raase, P., Raith, M., Ackermand, D., and Lal, R.K. (1986) Progressive metamorphism of mafic rocks from greenschist to granulite facies in the Dharwar Craton of South India. Journal of Geology, 94, 261–282.

Razakamanana, T., Ackermand, D., and Windley, B.F. (2000) Högbomite in migmatitic paragneiss in the Betroka shear belt, Vohidava area, Precambrian of southern Madagascar. Mineralogy and Petrology, 68, 257–269.

Rumble, D. III. (1976) Oxide minerals in metamorphic rocks. In: Mineralogical Society of America, Reviews in Mineralogy, Vol. 3, R1–24.

Sack, R.O. and Ghiorso, M.S. (1989) Importance of consideration of mixing properties in establishing an internally consistent thermodynamic data base: thermochemistry of minerals in the system Mg_2SiO_4-Fe_2SiO_4-SiO_2. Contributions to Mineralogy and Petrology, 102, 41–68.

Sack, R.O. and Ghiorso, M.S. (1991) Chromite as a petrogenetic indicator. In D.H. Lindsley, Ed., Oxide Minerals, vol. 25, 323–353. Reviews in Mineralogy, Mineralogical Society of America, Washington, D.C.

Seifert, F. (1974) Stability of sapphirine in the aluminous part of the system MgO-Al_2O_3-SiO_2-H_2O. Journal of Geology, 82, 173–204.

Sengupta, P., Sen, J., Dasgupta, S., Raith, M.M., Bhui, U., and Ehl, J. (1999) Ultrahigh temperature metamorphism of metapelitic granulites from Kondapalle, Eastern Ghats Belt: Implications for the Indo-Antarctic correlation. Journal of Petrology, 40, 1065–1087.

Serebriakov, N.S., Gladysheva, A.P., and Terehov, E.N. (2001): Plagioklasity korundovyh proyavlenij Severnoi Karelii: Hitoostrov, Varazkoe (Plagioclasites of corundum bearing localities of the North Karelia: Hitoostrov, Varazkoe). In: "Geology and geoecology of the Fennoscandian Shield, East-European platform and their surrounding," Abstr. XI Conference of young scientists, St. Petersburg, Russia, p. 28–30.

Serebriakov, N.S. and Aristov, V.V. (1999) Ob obrazovanii hitoostrovskogo proyavlenija corunda v Karelii (On the genesis of the Hitoostrov corundum-bearing exposure in Karelia) In Physical-chemical problems of geological processes. Internet Symposium on the honour of 100 anniversary of D.S. Korzhinsky, Moscow, Abstracts, p. 116–117.

Spear, F.S. (1993) Metamorphic phase equilibria and pressure-temperature-time paths. Mineralogical Society of America, Monograph Series, 799 pp.

Spear, F.S. and Rumble, D. III (1986) Pressure, temperature, and structural evolution of the Orfordville Belt, west-central New Hampshire. Journal of Petrology, 27, 1071–1093.

Teale, G.S. (1980) The occurrence of högbomite and taaffeite in a spinel-phlogopite schist from the Mount Painter Province of South Australia. Mineralogical Magazine, 43, 575–577.

Terehov, E.N. and Levitsky, V.I. (1991) Geological-structural systematics for the localisation of corundum mineralisation in NW Belomorian. Reports of High Education Institutes, Geology & Exploration, No. 6, 3–13.

Visser, D., Thijssen, P.H.M., and Schumacher, J.C., (1992) Högbomite in sapphirine-bearing rocks from the Bamble Sector, south Norway, Mineralogical Magazine, 56, 343–351.

Zakrzweski, M.A. (1977) Högbomite from the Fe-Ti deposit of Liganga (Tanzania). Neues Jahrbuch für Mineralogie Monatshefte, 1977, 373–378.

MANUSCRIPT RECEIVED AUGUST 3, 2003
MANUSCRIPT ACCEPTED JANUARY 19, 2004
MANUSCRIPT HANDLED BY JENNIFER THOMSON